Astron. Astrophys. 325, 228–236 (1997)

ASTRONOMY
AND
ASTROPHYSICS

HST-GHRS observations of candidate β Pictoris-like circumstellar gaseous disks*

A. Lecavelier des Etangs[1], M. Deleuil[2], A. Vidal-Madjar[1], A-M. Lagrange-Henri[3], D. Backman[4], J.J. Lissauer[5,6], R. Ferlet[1], H. Beust[3], and D. Mouillet[3]

[1] Institut d'Astrophysique de Paris, CNRS, 98 bis boulevard Arago, F-75014 Paris, France
[2] Laboratoire d'Astronomie Spatiale, CNRS, BP 8, F-13376 Marseille Cedex 12, France
[3] Groupe d'Astrophysique de Grenoble, CERMO BP53X, F-38041 Grenoble Cedex, France
[4] Physics and Astronomy Dept, Franklin and Marshall College, P.O. Box 3003, Lancaster PA 17604, USA
[5] Astronomy Program, Department of Earth and Space Sciences, State University of New York, Stony Brook NY 11794, USA
[6] Space Science Division, Mail Stop 245-3, NASA Ames Research Center, Moffett Field, CA 94035, USA

Received 28 August 1996 / Accepted 20 March 1997

Abstract. We present HST-GHRS observations of four stars in search of β Pictoris-like circumstellar gaseous disks. We detected gas around HR 10, HR 2174 and 51 Oph at large distances from the stars; this gas is circumstellar since the absorption lines from very excited levels require densities incompatible with those found in the diffuse interstellar medium. The shape of the lines and the Mg II doublet ratio give evidence that clumpy gas is continuously falling onto these stars. Possible interpretations are discussed.

Key words: stars: circumstellar matter; planetary systems – stars: β Pictoris – line: formation – ISM: clouds

1. Introduction

The particles surrounding main sequence stars discovered in the infrared with the IRAS satellite (Aumann et al. 1984) show common features offering indirect clues to the presence of other planetary systems in the universe. The dusty environments of these stars have been subject to detailed analyses (see the review by Backman & Paresce 1993). In the case of β Pictoris, the disk has been imaged with different techniques (Smith & Terrile 1984, Lecavelier des Etangs et al. 1993, Kalas & Jewitt 1995, Mouillet et al. 1997).

Since 1985, the gaseous component of the β Pictoris disk has been observed in both visible and UV lines with IUE and HST (see review by Ferlet & Vidal-Madjar 1995). The observed spectral signatures toward β Pictoris led to the explanation that the gas content was probably produced by the evaporation of many small bodies ranging from dust grains to kilometer-sized bodies. If true, that gas content may be simply the signature of larger bodies destroyed through collisions and evaporation, a situation that lasted $\sim 7 \cdot 10^8$ years in our own Solar System after it was formed (Soderblom et al. 1974).

In order to have a more complete comprehension of the general problem of planetary system formation and evolution, one needs to study several cases, in different states. Observations of a number of evolved circumstellar disks may provide clues toward understanding the diversity of planetary systems present in our galaxy (Lissauer 1993).

The gaseous counterpart of the dust disks was previously unambiguously identified only in the case of β Pictoris. It is thus of prime importance to search for the presence of gas in other circumstellar environments. This was started in the visible by Hobbs (1986). Lagrange-Henri et al (1990a) observed 49 stars in Ca II and Na I to look for spectral signatures similar to the ones observed in the case of β Pictoris. The result was that very few stars presented possible circumstellar gas. HR 10, HR 2174 and 51 Oph (HR 6519) were the three most intriguing stars observed in this survey. They merited observations with high resolution spectroscopy in the UV where stronger lines are available. We used the unique capabilities of GHRS in reaching good S/N at short wavelengths and a resolution similar to the one we have in the visible to further compare these objects. We selected some UV lines of these stars in order to confirm the existence of the circumstellar gas and to improve our knowledge of such gaseous disks.

As a first result the data revealed the presence of C I around 51 Oph with the HST-GHRS. Because 51 Oph is an emission line star (B9.5Ve) its infrared excess seems less surprising than for other main sequence stars and could *a priori* have been re-

Send offprint requests to: A. Lecavelier des Etangs

* Based on observations with the NASA/ESA *Hubble Space Telescope*, obtained at the Space Telescope Science Institute which is operated by the Association of Universities for Research in Astronomy Inc., under NASA Contract NAS5-26555.

lated to free-free emission. However, the 51 Oph far-infrared energy distribution definitely confirms that this emission is due to the presence of cold dust at distances $\gg$100 AU (Waters et al. 1988, Waelkens et al. 1996). The connection between the circumstellar absorption lines and the dust thermal emission was missing until our HST-GHRS detection of C I at 1560 Å connected to the cold, distant parts of the 51 Oph disk (Lecavelier des Etangs et al. 1997). This was the first result of our GHRS program designed to better constrain the gas content in systems with already known circumstellar absorption lines.

This paper mainly concerns the hot central parts of the gaseous disks, and detections of very excited species will be presented. The observations and data analysis are in Sect. 2. The results will be found in Sect. 3 and 4, and the discussion in Sect. 5.

2. Observations

2.1. Targets

In this paper we present new HST-GHRS spectra of the environments of four stars known to have some spectral similarities with β Pictoris. The selected stars were HR 10, HR 2174, 51 Oph (HR 6519) and ϵ Gru (HR 8675) (see Table 1).

The available data showed that HR 10, HR 2174 and 51 Oph exhibit clear similarities with β Pictoris. For example, redshifted variable absorption features similar to ones at β Pictoris have been observed toward HR 10 and 51 Oph (Lagrange-Henri et al 1990b). Similarly to β Pictoris, IUE revealed the presence of C IV around 51 Oph which cannot be explained by stellar photoionization (Grady et al. 1989, Grady & Silvis 1993). In addition, these IUE observations of 51 Oph showed the presence of spectroscopic variations very similar to the β Pictoris ones (for comparison with β Pictoris IUE spectra see Deleuil et al. 1993) as well as accretion of over-ionized species. All these components are the signature of warm, collisionally ionized gas and accreting material, and may be linked to the Falling-Evaporating-Bodies (FEB) phenomenon observed around β Pictoris (Beust et al. 1990, Ferlet & Vidal-Madjar 1995). Dust has been detected around 51 Oph (Coté & Waters 1987), and HR 10 presents an IR excess consistent with free-free emission and some small amount of circumstellar dust (Cheng et al. 1991).

In addition, from an optical survey of the interstellar absorption due to the local cloud, one star (ϵ Gru) has shown Ca II circumstellar-like lines at the stellar velocity (~ -1 km s^{-1}) and without a Na I counterpart (Bertin et al. 1993). We thus decided to add this star to our target list.

2.2. Lines

To detect the gaseous part of the disks and to have a view of the physical state of the circumstellar material around the selected stars, we looked at the following very strong UV lines with the Small Science Aperture (SSA) and ECH-B:

- Fe II line from the ground level,
- Fe II fine structure lines at 2598.4Å (385 cm^{-1}) and 2607Å (667 cm^{-1}),
- Mn II multiplet at 2600Å and numerous very excited Fe II lines in the same domain,
- the very strong Mg II doublet at 2802.7Å and 2795.5Å.

Absorptions from excited fine-structure levels require densities incompatible with those found in the interstellar medium toward these nearby stars ($d < 100$ pc). If detected, the presence of absorption from Fe II excited levels is thus a strong signature of the circumstellar origin.

In addition, we obtained a G160M spectrum at the end of each orbit dedicated to the two brightest stars (51 Oph and ϵ Gru). We observed the 1550Å region to search for CO, C I and C IV signatures. This allowed us not only to detect C I around 51 Oph enabling us to evaluate the connection between gas and dust (more precisely between C I and infrared excess, Lecavelier des Etangs et al. 1997), but also to probe again the C IV lines observed with IUE by Grady & Silvis (1993). These IUE observations showed strong C IV variations with highly redshifted absorption ($v \sim 100$ km s^{-1}).

Table 1. Summary of the target characteristics. v_r^* are the stellar radial velocities given by Hoffleit (1982).

Star	m_v	Type	$v \sin i$ (km s^{-1})	v_r^*
HR 10	6.2	A6V	195	
HR 2174	5.7	A3V	250	+34
HR 6519 51 Oph	4.8	B9.5Ve	220	-12
HR 8675 ϵ Gru	3.4	A3V	236	+0

Table 2. Log of observations. Four orbits were used to observe four different stars. Spectra around 1550Å were obtained with the Grating G160M, the others with ECH-B.

Star	Lines	Wavelength (Å)	exp. time (s)
HR 10	Fe II	2597-2610	326.4
	Mg II	2793-2808	389
HR 2174	Fe II	2597-2610	326.4
	Mg II	2793-2808	391
HR 6519	CO , C I, C IV	1530-1570	252
51 Oph	Fe II	2597-2610	108.8
	Mg II	2793-2808	108.8
HR 8675	CO, C I, C IV	1530-1570	407
ϵ Gru	Fe II	2597-2610	108.8
	Mg II	2793-2808	108.8

2.3. Observations

The observations were obtained between July 1995 and February 1996. They were done with the oversampling mode which samples four data points per resolution element, exposure times necessary to reach S/N ratios between 20 and 50, and with the SSA aperture which gives a better spectral resolution (Table 2). All data were also gathered in the "fp-split" mode, which splits the total exposure time in four sub-exposures at four different

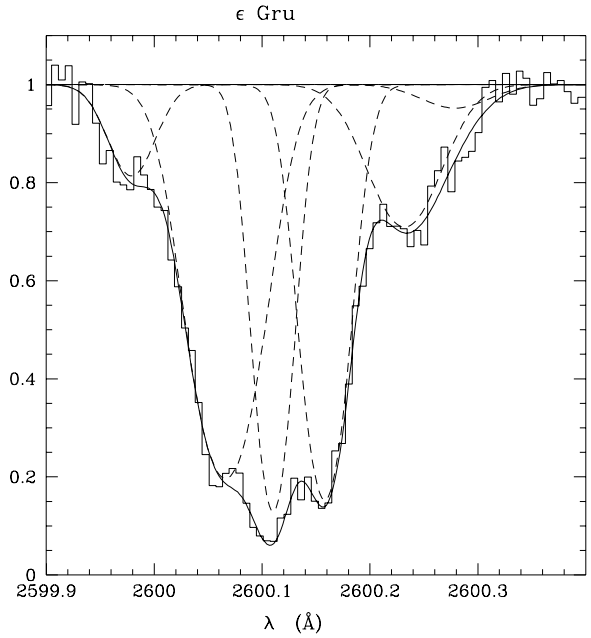

Fig. 1. Fe II line (λ_0=2600.173Å) toward ϵ Gru. The fit has been obtained with Voigt profiles. At least six components are necessary to obtain a good fit.

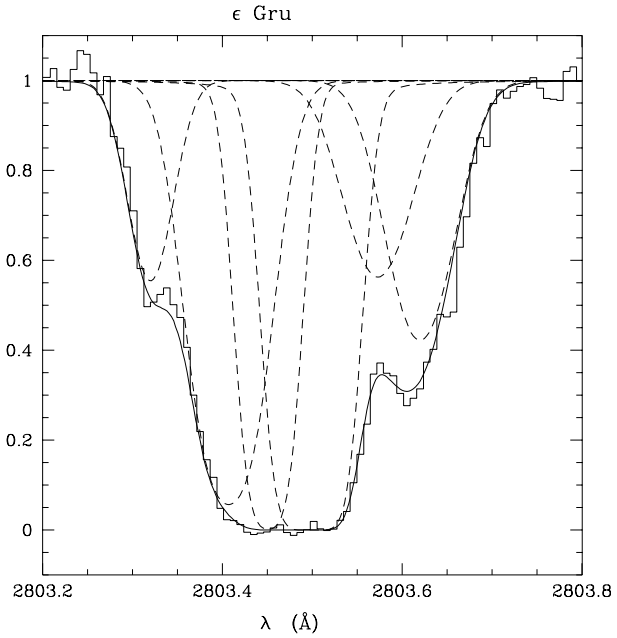

Fig. 2. Mg II line (λ_0=2803.531Å) toward ϵ Gru. The fit has been obtained with the same components as in the previous figure.

Table 3. List of the lines observed toward ϵ Gru. All these lines are from the nearby interstellar medium ($d < 23$ pc).

	Velocity (km s^{-1})	N(Mg II) (cm^{-2})	N(Fe II) (cm^{-2})	b (km s^{-1})
I	-22.4	1.6 10^{12}	8.2 10^{11}	3.0
II	-12.3	1.1 10^{13}	8.9 10^{12}	4.4
III	-7.3	8.9 10^{13}	7.2 10^{12}	2.0
IV	-1.7	3.1 10^{14}	7.1 10^{12}	2.6
V	6.8	2.4 10^{12}	2.1 10^{12}	5.0
VI	12.2	3.4 10^{12}	2.8 10^{11}	4.7

positions of the grating in order to decrease the noise from the photocathode granularity. The four different shifts have been estimated by cross-correlation with *IDL* software.

2.4. Reductions

The continua and line profiles have been determined following the procedure defined by Lemoine et al. (1995). The continua of the spectra were fitted by a polynomial with degree determined by a cross-validation method. This method gives the "best" degree of fit to the continuum information without fitting the noise (see Lemoine et al. 1995 for a detailed explanation). The parameters of the fits by Voigt profiles were obtained by a search for χ^2 minimum in the parameter space with a simulated annealing (Metropolis et al. 1953).

3. ϵ Gru

3.1. The absorptions lines

As already stated, ϵ Gru was selected from the results of a survey dedicated to the local interstellar medium. The possible circumstellar origin of the observed gaseous absorption had to be checked through UV lines.

In the spectrum around 2600Å, we only detected the Fe II line from the ground level. Profile fitting provides a set of at least six components (Fig. 1). These components are also detected in Mg II lines (Fig. 2 and Table 3). In terms of velocities, the three strongest absorptions are in good agreement with the three components of the local interstellar medium detected from the observations of Ca II lines at -13.0, -7.0 and -1.1 $\pm$1.5 km s^{-1} (Bertin et al. 1993) and in particular the component at -7 km s^{-1} corresponds to the absorption due to the "Local Interstellar Cloud".

3.2. The Mg II ratio

The ratio of the Mg II doublet lines can give information on the size of absorbing clouds in comparison to the size of the star. In order to analyze this ratio, we simply divided spectra obtained after the fitting of the continuum by a first or a second degree polynomial (it has been extensively checked that the results presented in this paper do not depend on the assumed fit of the continuum).

The basis of this division is very simple: as the ratio of the oscillator strengths is exactly 2, if a cloud covers the whole stellar surface seen from the Earth, we obtain two lines with profiles: $f_h = e^{-\tau}$ and $f_k = e^{-2\tau}$. Then, the ratio of the two

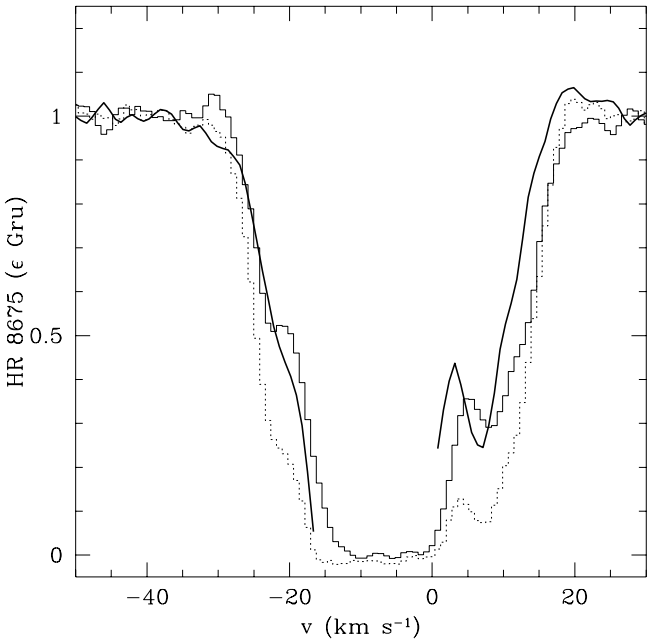

Fig. 3. Ratio of the Mg II doublet lines (thick solid line, which cannot be evaluated at the bottom of the absorption feature where the flux is too faint). The dotted line represents the Mg II k line. The thin solid line gives the Mg II h line, which is the faintest absorption of the doublet. The latter must follow the ratio if the ratio is normal. In other words, since interstellar absorption covers all the stellar surface, the ratio must have the same profile as the faintest absorption line (Sect. 3.3). The ratio is obviously normal in the case of the absorptions observed toward ϵ Gru. This provides an useful comparison for the other stars in which abnormal ratios are found.

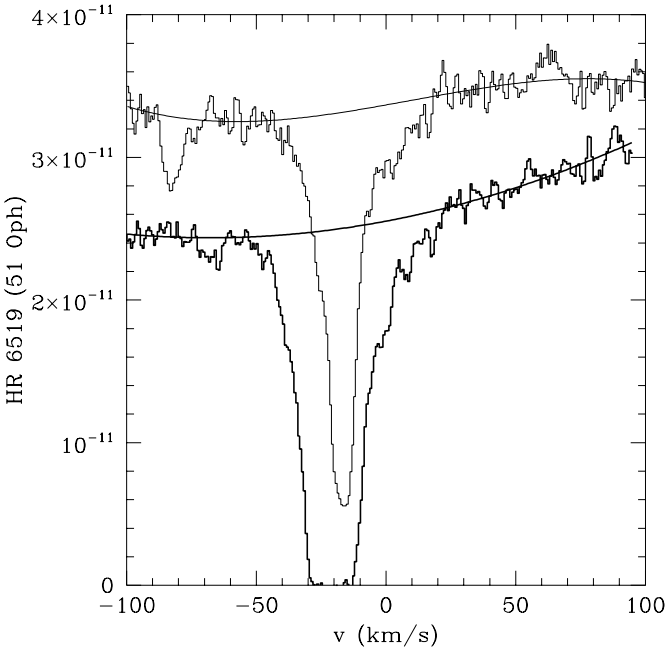

Fig. 4. Lines from the ground level of Fe II (thick line, λ_0 = 2600.17Å) and from J levels at 668 cm^{-1} (thin line, λ_0 = 2607.87Å) observed toward 51 Oph. For clarity, the line from J level has been shifted upward by 0.5×10^{-11} erg s^{-1} cm^{-2}. The fits to the continua were determined by a polynomial with a cross-validation method.

lines is $f_k/f_h = e^{-\tau} = f_h$. The profile of the ratio must be similar to the profile of the Mg II h line.

In contrast, if the cloud is optically thick but small, covering only a fraction F of the stellar surface, then we have: $f_h = f_k = (1 - F) \neq 0$. In that case, the ratio of the two lines is: $f_k/f_h = 1 \neq f_h$. The profile of the ratio is then equal to one and is different than the profile of the faintest line.

The Mg II doublet components in the ϵ Gru spectrum present the expected normal ratio (Fig. 3). This shows that the observed absorbing clouds are larger than the star.

3.3. Conclusion

In summary, the spectra show:

- There are no Fe II lines from any excited levels.
- No signatures of either CO, C I nor C IV were observed.
- The shape of all absorption lines are symmetric.
- All of the observed components in the Mg II doublet present the normal ratio.

Finally, the negative result for this star provides a very useful reference for the three other stars which greatly differ on these four points.

4. HR 10, HR 2174 and 51 Oph

For the three other stars (HR 10, HR 2174 and 51 Oph), we have detected a large number of lines from excited levels. In particular for Fe II lines, we see a lot of narrow absorption lines which cannot be either photospheric lines which must be rotationally broadened, nor interstellar ones, since the excited fine-structure levels require densities incompatible with those found in the local interstellar medium (see ϵ Gru for comparison). Table 4 shows all the detected lines and their equivalent widths. Some examples of Fe II lines from levels with high excitation energy (E_l) can be found in Figs. 5 to 8.

The presence of these excited states of the Fe II ions is not surprising in these stars classified as *shell stars*. However the very narrow lines ($\Delta v \sim 20$ km s^{-1}) with sharp absorption in contrast to the rotationally broadened stellar lines indicates that the gas may be at relatively large distances ($\gtrsim 15 R_*$). This discontinuity between the stellar spectra and the gaseous absorption is clearly detected at the resolution given by GHRS and does not depend on the assumed continuum (Fig 4). Moreover, as already noted (Abt & Moyd 1973), the very large $v \sin i$ for all of these stars gives evidence that the detected gas is near the equatorial plane, maybe in a disk-like geometry.

For each of the three stars 51 Oph, HR 10 and HR 2174, the conclusion is similar: we have confirmed the presence of excited Fe II ions of circumstellar origin. However, in detail, each star presents different characteristics (Table 4) and shows

Table 4. Lines observed in spectra of 51 Oph, HR 10 and HR 2174

						51 Oph				HR 10				HR 2174			
		λ_0 (Å)	$\log(gf)$	f	E_l (cm^{-1})	λ (Å)	v (km.s^{-1})	W (Å)	N (cm^{-2})	λ (Å)	v (km.s^{-1})	W (Å)	N (cm^{-2})	λ (Å)	v (km.s^{-1})	W (Å)	N (cm^{-2})
Si	II	1533.431	-0.288	0.1288	287.24	1533.34	-18	0.25	a								
C	IV	1548.195	-0.418	0.1888	0.00	1548.19	-1	0.42	a								
C	IV	1550.770	-0.720	0.0946	0.00	1550.75	-4	0.30	a								
Fe	II	1559.085	-0.269	0.05382	1872.57	1559.00	-17	0.050	4.3×10^{13}								
Fe	II	1560.251	-1.185	0.005443	2430.10	c	-19		4.4×10^{13}								
C	I	1560.309	-1.095	0.08041	0.00	d	-15		1.2×10^{13}								
C	I	1560.682	-0.743	0.06030	16.40	d	-15		1.1×10^{13}								
C	I	1560.709	-1.220	0.02010	16.40	d	-15		1.1×10^{13}								
Fe	II	1563.790	-0.202	0.07851	2430.10	1563.68	-19	0.067	4.4×10^{13}								
Fe	II	1566.822	-0.416	0.038371	1872.57	1566.71	-21	0.05	6.0×10^{13}								
Fe	II	2599.146	-0.100	0.09929	384.79	2599.005	-17	0.14	a	2599.27	14	0.11	a	2599.44	34	0.22	a
Fe	II	2600.173	0.350	0.2239	0.00			0.26	b			0.21	b			0.25	b
e														2606.06	-3[e]	0.006	
Fe	II	2606.089	-0.180	0.165173	36126.39		not	detected		2606.29	23	0.022	2.2×10^{12}	2606.34	29	0.020	2.0×10^{12}
e														2606.45	42[e]	0.025	
Mn	II[f]	2606.462	0.130	0.1927	0.00	2606.30	-18	0.082	7.1×10^{12}	2606.57	13	0.050	4.3×10^{12}	2606.69	26	0.11	9.5×10^{12}
Fe	II	2607.296	0.040	0.182746	36252.92	2607.16	-16	0.025	2.3×10^{12}	2607.41	13	0.015	1.3×10^{12}	2607.55	29	0.055	5.0×10^{12}
Fe	II	2607.866	-0.170	0.1127	667.68	2607.72	-17	0.14	2.0×10^{13}	2607.98	13	0.07	1.0×10^{13}	2608.11	28	0.16	2.4×10^{13}
Fe	II	2794.710	-0.870	0.01349	25805.33		not	detected		2794.83	13	0.015	1.6×10^{13}	2794.98	29	0.036	3.9×10^{13}
Mg	II	2796.352	0.088	0.6123	0.00			0.39	b			0.32	b			0.34	b
Fe	II	2798.742	-1.480	0.003311	26352.77	2798.6	-15	0.004	2.7×10^{13}		not	detected		2799.00	28	0.008	3.5×10^{13}
Fe	II	2800.120	-1.000	0.010000	26352.77	2800.003	-13	0.006	8.6×10^{12}	2800.25	14	0.008	1.2×10^{13}	2800.39	29	0.030	4.3×10^{13}
Fe	II	2800.195	-1.674	0.003531	36252.92		not	detected			not	detected		2800.50	33	0.006	2.4×10^{13}
Mg	II	2803.531	-0.214	0.3054	0.00			0.38	b			0.28	b			0.31	b

a: Obviously saturated.
b: Saturated and blended with interstellar absorption.
c: Determined by Profile fitting of the FeII component at λ_0=1563.79Å (Lecavelier des Etangs et al. 1996).
d: Determined by Profile fitting of the CI multiplet.
e: Unidentified. Velocity has been determined assuming that the line is from FeII at λ_0=2606.089Å.
f: MnII has probably a circumstellar origin (not detected toward ϵ Gru).

unambiguous detection of low velocity accreting gas when IUE would indicate quiescence.

4.1. 51 Oph

The circumstellar gaseous absorptions toward 51 Oph have been found with a radial velocity of $v_r^g = -17\pm1$ km s^{-1} (Fig. 5). Heliocentric velocities are consistent within ±3 km s^{-1} for the spectrum around 1550Å with a resolving power of 30 000, and within ±1 km s^{-1} for the spectrum around 2600Å with a resolving power of 80 000. The radial velocities measured in the spectrum around 2800Å seem to present a systematic error, which may be due to the HST internal wavelength calibration; thus no conclusion can be extracted from them.

The obtained gas radial velocity is not very different from the stellar radial velocity given by Hoffleit (1982) ($v_r^* = -12$ km s^{-1}). It is possible that the small difference can be due to the presence of redshifted absorptions like the ones observed by Grady & Silvis (1993) (see also the C IV lines in Sect. 4.1.1).

We conclude that the gaseous components have been observed at very small radial velocities relative to the star, except for the C IV lines observed with a systemic redshift of $\sim$ +15 km s^{-1} relative to the other lines. The non-detection of strongly redshifted components and the symmetric shape of the Fe II lines show that 51 Oph has been observed during a quiet period. Other observations are necessary to make conclusions about the lines which are observed with IUE at high redshifted velocities.

4.1.1. C IV lines

C IV had already been detected around 51 Oph (Grady & Silvis 1993). The presence of this ion is very surprising since the stellar flux is unable to ionize C III (the ionization potential of C III is 65 eV). In addition, the difference between the observed radial velocities shows that this gas cannot be supplied by the stellar atmosphere. Excitation by collisions is necessary as the origin of this ionization.

In contrast to Grady & Silvis (1993), we observed only rather symmetrical absorption lines, at relatively small radial velocities. This confirms that 51 Oph was probably observed in a quiescent phase. We only note a very small anomaly in the ratio of the two C IV lines, which could be explained by an optically thick cloud smaller than the stellar size (Fig. 6).

4.2. HR 10

All of the absorptions toward HR 10 have been found with a radial velocity of $v_r^g = 14\pm1$ km s^{-1}, except for a component at λ = 2606.3Å. If this line is from the excited level of Fe II at rest wavelength λ_0 = 2606.09Å, then its radial velocity is 23 km s^{-1}. But it is not excluded that this line is an unidentified line, similar to the line observed at λ = 2606.45Å toward HR 2174.

The lines from ground and excited levels of Fe II are represented in Fig. 7. We see that the lines from excited levels are very asymmetric and present a very sharp drop on the blue side and a broader shape on the red side. It seems that the gas is

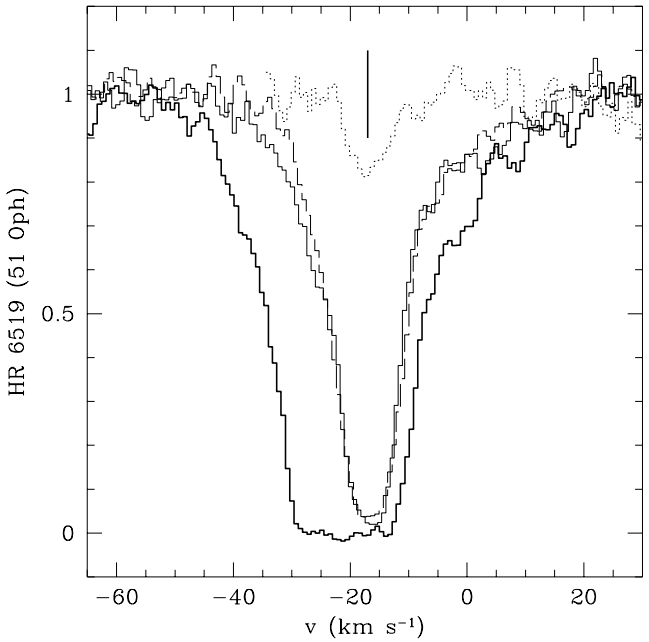

Fig. 5. Lines from the ground level of Fe II (thick line, λ_0 = 2600.17Å) and from J levels (thin lines): at 385 cm^{-1} (thin dashed line, λ_0 = 2599.15Å) and 668 cm^{-1} (thin solid line, λ_0 = 2607.87Å) observed toward 51 Oph. Absorptions from the ground level are visible at velocities smaller and larger than absorptions from excited levels. They probably have an interstellar origin. The lines from the J levels are at the mean gas radial velocity, which is marked by the vertical tick (v_r^g = −17 km s^{-1}). These lines are rather symmetric, which must be compared to the shape of the lines toward HR 10 and HR 2174. The dotted line is an absorption from a very excited level of Fe II at 36 253 cm^{-1} (λ_0 = 2607.3Å).

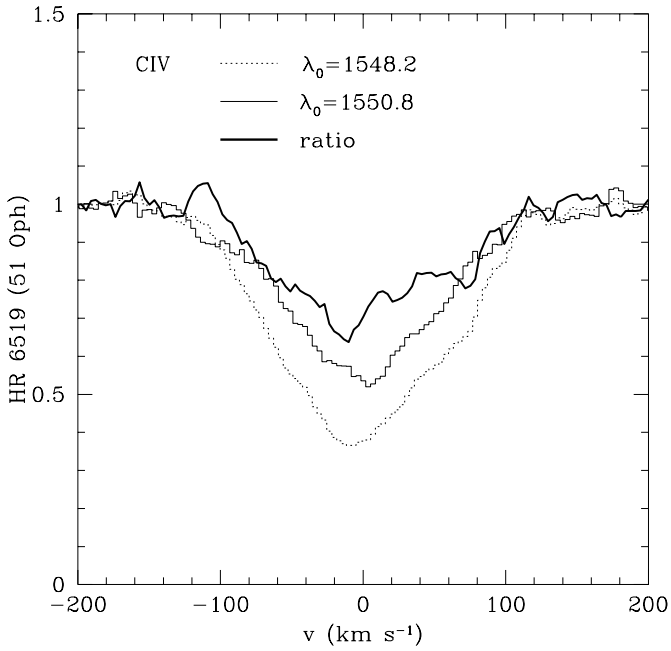

Fig. 6. C IV lines toward 51 Oph (thin and dotted lines) and their ratio (thick line). We first see that the profile of the ratio is rather similar to the faintest line, which shows that the line ratio is approximately normal. However, in detail, we see that between 0 and 60 km s^{-1} the observed ratio is larger than the expected one. If real, this could be explained by an optically thick absorption which covers only a fraction of the stellar surface and moves toward the star. This absorption may explain the difference in the radial velocities between the C IV and other lines.

falling onto the star. This presents certainly similarities with the β Pictoris case.

4.3. HR 2174

HR 2174 is certainly the most interesting candidate among the three stars for which gas has been detected. First, it shows many lines from very excited levels of Fe II with large equivalent widths (Table 4). For example, the line from the level with excitation energy 36 253 cm^{-1} is shown in Fig. 8.

Moreover, as in the case of HR 10, these lines are very asymmetric, again with very sharp blue sides. For the blue side of the spectra, the profile of the Fe II line from 385 cm^{-1} is very similar to the profile of the line from 668 cm^{-1}. This is expected because these two lines have about the same oscillator strength. However, the red sides are very extended with redshifted absorptions at velocities up to 40 km s^{-1} relative to the stellar velocity. In this region of the spectra, the two lines from J levels represented in Fig. 8 are different: the 668 cm^{-1} level is less populated than the 385 cm^{-1} level. This difference has already been observed in spectra of β Pictoris for redshifted absorptions at very large velocities (See Fig. 9 for a spectrum of Fe II lines toward β Pictoris).

Again, it seems that matter is also continuously falling onto this star.

As for 51 Oph, we see that the gaseous radial velocity (v_r^g = 28 km s^{-1}) is smaller by about 6 km s^{-1} than the stellar radial velocity. This difference may not be significant if an error is present in the HST calibration (but wavelengths are consistent in the case of ϵ Gru), or if the radial velocities given by Hoffleit (1982) are inaccurate for these stars with very large $v \sin i$.

4.4. Abnormal Mg II ratio

As demonstrated in Sect. 3.2, the comparison of the profile of the Mg II ratio and the profile of the faintest line allows us to make conclusions about the size of the absorbing clouds. In the cases of HR 10, HR 2174 and 51 Oph, Fig. 10 clearly shows that the ratios are normal on the blue sides of the interstellar absorptions lines. But on the red sides, the lines have absorptions which do not follow the oscillator strength ratio. The observed ratios are very close to 1. The clouds of matter falling onto these stars are thus optically thick and must have characteristic sizes smaller than the projected sizes of the stars, as is the case for β Pictoris also shown in Fig. 10.

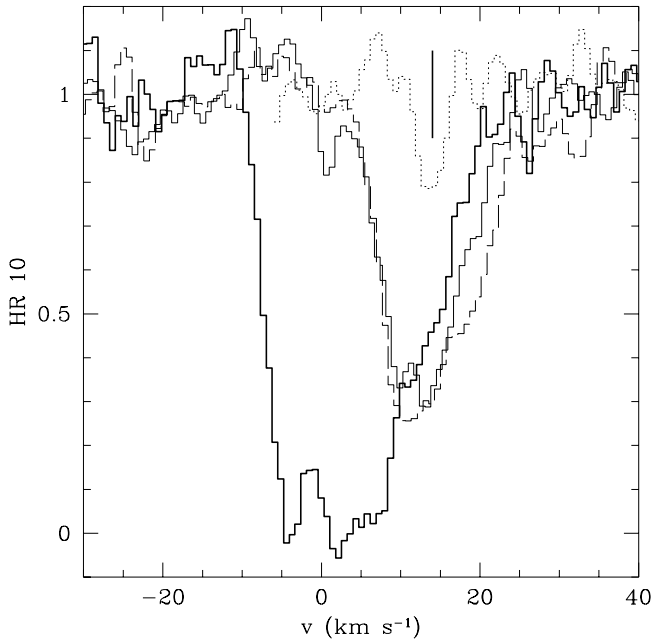

Fig. 7. Same as Fig. 5 but with the spectrum of HR 10. Here the lines of excited Fe II are very asymmetric and present a tail of absorptions at redshifted velocities.

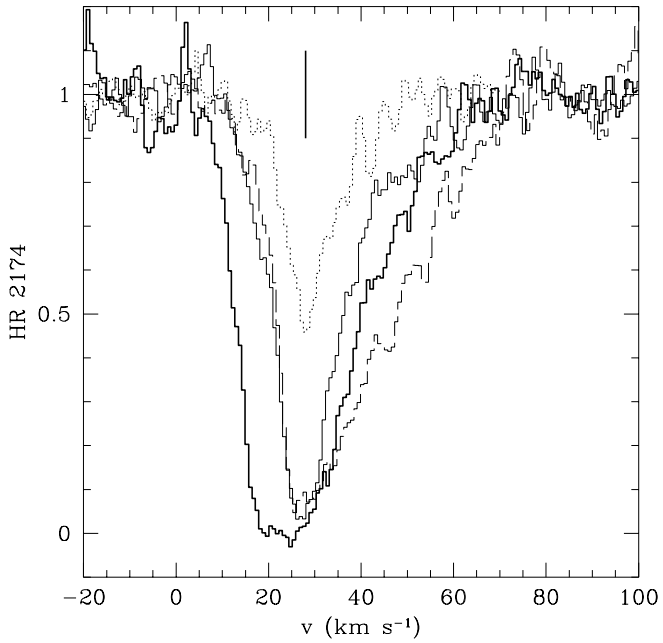

Fig. 8. Same as previous figure but with the spectrum of HR 2174. Lines from excited levels of Fe II are very strong and asymmetric. The dotted line representing Fe II from a level at 36 253 cm^{-1} (4 eV) is particularly deep. The vertical tick shows the gaseous radial velocity v_r^g = 28 km s^{-1}

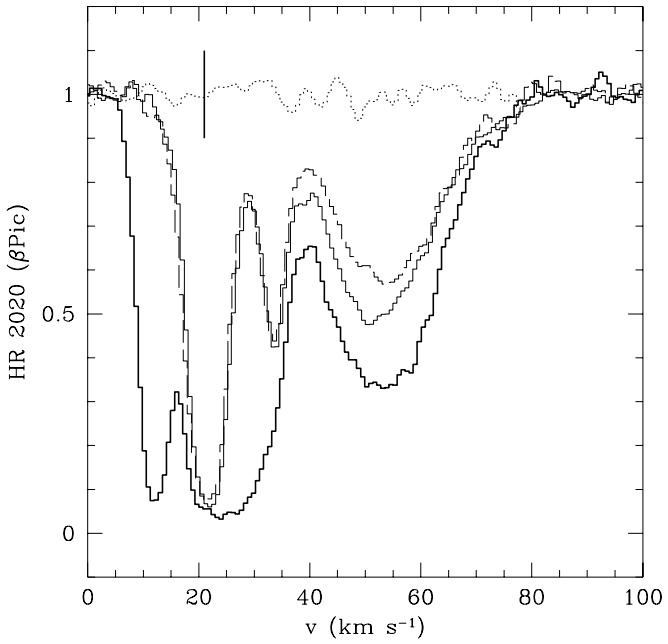

Fig. 9. Same as previous figures but with a spectrum of β Pictoris obtained by Vidal-Madjar et al. (1994). There are no lines of Fe II from the level at 36 253 cm^{-1}, however Fe II lines from excited levels up to 21 000 cm^{-1} have already been detected. In other lines, numerous components are visible. The first one at 10 km s^{-1} probably has an interstellar origin without detection from J levels. The absorption at 21 km s^{-1} is from the stable component of the gaseous disk. Absorptions up to 80 km s^{-1} are very sporadic and explained as due to Falling-Evaporating-Bodies (Beust et al. 1990). The difference in absorption of the different J levels of Fe II may have similar origin in the other observed stars.

5. Discussion

The presented GHRS observations show that accreting activity is detected even at epochs when the lower resolution IUE data would indicate an absence of such falling gas. Moreover the line ratio analysis showed the clumpy structure of the falling material. We now have three additional stars with circumstellar gas and redshifted absorptions lines explained by *clumpy* gas falling onto these stars. On the other hand, infalling gas has also been detected in lower resolution spectra of Herbig Ae/Be stars (Perez et al. 1993), UX Orionis (Grinin et al. 1997), post Herbig Ae/Be stars and shell stars (Grady et al. 1996). These observations raise an important problem. The absorptions observed for ten years in the β Pictoris spectra are very well explained by the Falling-Evaporating-Bodies scenario. But in that scenario, the events are always redshifted because the longitude of the periastron of the falling bodies is always the same (see discussion in Beust et al. 1996). However, it would be surprising that the direction of the periastron of the gas parent bodies is always toward the Earth.

To solve this paradox, it has been proposed that the bodies can be completely evaporated before their periastron, and thus give only redshifted absorptions (see for example Ferlet

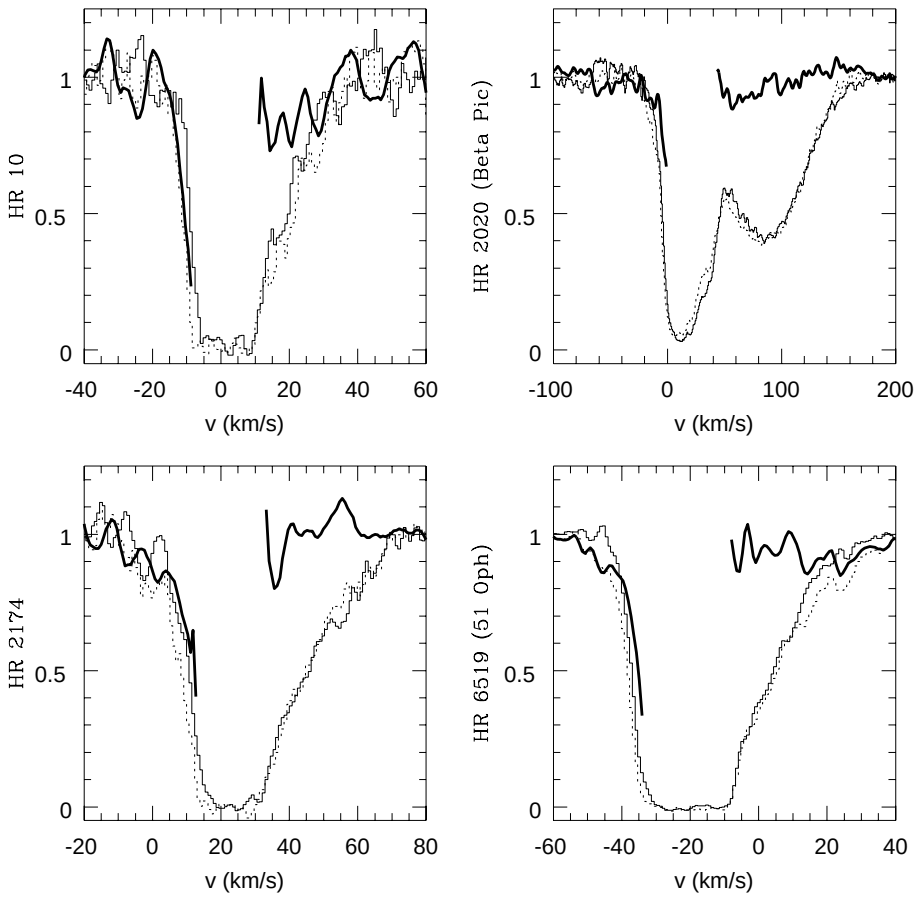

Fig. 10. Ratio of the Mg II doublet lines (thick solid line). The velocity scale is the same for all the stars except for β Pictoris with a velocity range chosen to be three times larger than for the program stars. The thin solid line gives the faintest absorption of the doublet (h line), which must follow the ratio if the ratio is normal (i.e. if the absorbing cloud covers all the stellar surface). The dotted line represents the k line of the Mg II doublet. As in the case of the interstellar absorptions observed toward ϵ Gru, the ratios are obviously normal in the blue part of the absorptions observed in the three target stars and in β Pictoris. But toward these stars, we observe that the ratio is equal to 1 for the redshifted absorptions. We conclude that there is gas moving toward these stars and covering only a fraction of the stellar surface (the β Pictoris spectrum is from Vidal-Madjar et al. 1994).

et al. 1987, Grinin et al. 1997). The observations presented in that paper strengthen this hypothesis. The phenomena observed around HR 10, HR 2174 and 51 Oph can be explained by evaporation of very small bodies, from dust to meteorites, continuously falling onto these stars.

This does not exclude the possibility that in the case of β Pictoris, the individual events observed with very high redshifted velocities can be due to larger bodies, which can survive after the periastron, but with always the same longitude of periastron. Up to now, these types of events have only been observed in the spectra of β Pictoris which is obviously a remarkable star.

One can believe that the presence of dust is a crucial test of the evaporating bodies scenario. As mentioned previously, 51 Oph shows an IR excess due to dust thermal emission (Waters et al. 1988); HR 10 IR excess is consistent with free-free emission and some small amount of circumstellar dust (Cheng et al. 1991); an IR excess for HR 2174 is possible but still to be confirmed (Lagrange et al. 1990a). However, even in cometary scenario, there is no direct connection between the presence of dust and infalling material. The dust produced at the same time as the gas by Falling-Evaporating-Bodies on very eccentric orbits is quickly expelled by radiation pressure on hyperbolic orbits. The presence of dust at large distances is more probably connected to collision or slow evaporation of bodies in nearly circular orbits at very large distances from the star ($d > 10\ AU$) (Weissman 1984). The evaporation of Orbiting-Evaporating-Bodies has been proposed to explain the CO detection and the dust distribution in the β Pictoris disk (Vidal-Madjar et al. 1994, Lecavelier des Etangs et al. 1996) and has a solar System analog with the evaporation observed at large distances on Chiron (Luu & Jewitt 1990) or Hale-Bopp (Sekanina 1996). As the falling bodies model does not imply the presence of a very large amount of dust, the absence of dust (as observed for HD 93563 by Grady et al. 1991) does not invalidate this model. One crucial test could be an abundance analysis which is expected to give abundances different from the cosmic ones and information on the place where the condensation and evaporation of the material take place (Lagrange et al. 1997).

References

Abt H.A., Moyd K.I., 1973, ApJ 182, 809
Aumann H.H., Gillett F.C., Beichman C.A., et al., ApJ 278, L23
Backman D.E., Paresce F., 1993, in *Protostars and Planets III*, E.H. Levy and J.I. Lunine Eds., Univ. of Ariz. Press, pp. 1253–1304
Bertin P., Lallement R., Ferlet R., Vidal-Madjar A., 1993, A&A 278, 549
Beust H., Lagrange-Henri A.M., Vidal-Madjar A., Ferlet R., 1990, A&A 236, 202
Beust H., Lagrange-Henri A.M., Vidal-Madjar A., et al., 1996, A&A, in press
Cheng K.P., Grady C.A., Bruhweiler F.C., 1991, ApJ 366, L87
Coté J., Waters L.B.F.M., 1987, A&A 176, 93

Deleuil M., Gry C., Lagrange-Henri A.M., et al., 1993, A&A 267, 187
Ferlet R., Hobbs L.M., Vidal-Madjar A., 1987, A&A 185, 267
Ferlet R., Vidal-Madjar A., 1995, *in* Circumstellar Dust Disk and Planet Formation (10$^{\rm th}$IAP meeting), Editions Frontières
Grady C.A., Bjorkman K.S., Snow T.P. et al., 1989, ApJ 339, 403
Grady C.A., Bruhweiler F.C., Cheng K.P., Chiu W.A., Kondo Y., 1991, ApJ 367, 296
Grady C.A., Silvis J.M., 1993, ApJ 402, L61
Grady C.A., Perez M.R., Talavara A., et al., 1996, ApJ 471, L49
Grinin V., Natta A., Tambovtseva L., 1997, A&A, in press
Hobbs L.M., 1986, ApJ 308, 854
Hoffleit D., 1982, The Bright Star Catalogue, 4^{th} revised version, Yale University Press.
Kalas P., Jewitt D., 1995, AJ 110, 794
Lagrange A.M, Ferlet R., Vidal-Madjar A., et al., 1990a, A&AS 85, 1089
Lagrange-Henri A.M., Beust H., Ferlet R., Hobbs L., Vidal-Madjar A., 1990b, A&A 227, L13
Lagrange A.M. et al., 1997, in preparation.
Lecavelier des Etangs A., Perrin G., Ferlet R., et al., 1993, A&A 274, 877
Lecavelier des Etangs A., Vidal-Madjar A., Ferlet R., 1996, A&A 307, 542
Lecavelier des Etangs, A., Vidal-Madjar, A., Backman, D.E., et al., 1997, A&A Letters, in press
Lemoine M., Ferlet R., Vidal-Madjar A., 1995, A&A 298, 879
Lissauer J.J., 1993, Ann. Rev. Astron. Astrophys. 31, 129
Luu J.X. & Jewitt D.C., 1990, AJ 100, 913
Metropolis N., Rosenbluth A., Rosenbluth M., Teller A., Teller E., 1953, J. Chem. Phys. 21, 1087
Mouillet D., et al., 1997, submitted
Perez M.R., Grady C.A., Thé P.S., 1993, A&A 274, 381
Sekanina Z., 1996, A&A 314, 957
Soderblom L.A., Condit C.A., Wes R.A., Herman B.M., Kreidler T.J., 1974, Icarus 22, 239
Smith B.A., Terrile R.J., 1984, Sci 226, 1421
Vidal-Madjar A., Lagrange-Henri A.M., Feldman P.D., et al., 1994, A&A, 290, 245
Waelkens C., Waters L.B.F.M., Graauw M.S., 1996, A&A 315, L245
Waters L.B.F.M., Coté J., Geballe T.R., 1988, A&A 203, 348
Weissman P.R., 1984, Science 224, 987

This article was processed by the author using Springer-Verlag LaTeX A&A style file *L-AA* version 3.